Coastal Dynamics 2017
Paper No. 023

MORPHODYNAMIC RESPONSE OF THE DEBEN ESTUARY TO FUTURE EXTREME WAVE CHANGE

Yunzhu Yin[1], Harshinie Karunarathna[2], Dominic E. Reeve[3]

Abstract

This paper investigates the morphodynamic response of the Deben Estuary, which is located in the southeast of the United Kingdom (UK), to possible extreme wave change in the future. The 1 in 100-year extreme wave condition derived from global climate simulations from the MRI-GCM3,2H model has been used. Three different representative bathymetry states of the estuary were selected for investigating the sensitivity of these bathymetries to storm wave change in the future. By examining the results, the morphological state most vulnerable to extreme wave change has been highlighted. The bathymetry states' responses to future extreme wave conditions under spring tide conditions have also been investigated and the difference in the morphological changes in each state due to the extreme wave change between present and future scenarios are presented.

Key words: Deben Estuary, sediment transport, morphodynamics, extreme wave change, numerical modelling, sensitive analysis

1. Introduction

The Deben Estuary, (Figure 1), is one of the most morphodynamically active estuaries in the UK with tide-dominated features (Posford Duvivier, 1999; HR Wallingford, 2002; Burningham and French, 2006). Apart from the tidal impacts, the estuarine system is also affected by high energy waves at the mouth of the estuary (Burningham and French, 2006; DEFRA, 2008). Future changes in wave climate due to global climate change may induce different morphodynamic responses that will be important for the long-term policy makers so that they can manage estuary in a sustainable manner (Arnott, 1968; Taylor et al., 2004; Beardall et al., 1991). To investigate the response of this system to future extreme wave changes, a computational morphological model was used in this study taking into account different initial bathymetry states.

The paper is structured as follows: Section 2 discusses the numerical modelling method used in this study, followed by a simple description of future extreme wave change which is used as the boundary condition for the numerical model. The modelling results are discussed in Section 3 and the paper is concluded in Section 4.

2. Methodology

The Delft 3D coastal area modelling suite (Booij et al., 1999; Lesser et al., 2004) is used in this study to investigate extreme wave change impacts on the morphology of the Deben Estuary. This coupled model has been well-validated in many applications of morphodynamic simulation, including those of Lesser et al. (2000), Dissanayake (2011) and van der Wegen and Roelvink (2012).

2.1. *Numerical models*

[1]College of Engineering, Swansea University, United Kingdom. y.yin744767@swansea.ac.uk
[2]College of Engineering, Swansea University, United Kingdom. H.U.Karunarathna@swansea.ac.uk
[3]College of Engineering, Swansea University, United Kingdom. D.E.Reeve@swansea.ac.uk

For the hydrodynamic and morphodyanmic modules, a nested depth-averaged Delft 3D model is used to introduce the hydrodynamic boundary conditions from deep ocean while waves were modelled using the third-generation wave module SWAN (Booji et al., 1999), considering random waves with a JONSWAP spectrum (Hasselmann et al., 1973). The SWAN grids are shown in Figure 2. In this study, in order to reduce the computational time, stationary waves were used. In this mode of operation, it is assumed that the time of waves propagating through the region is not important for the application (Delft3D Wave User Manual).

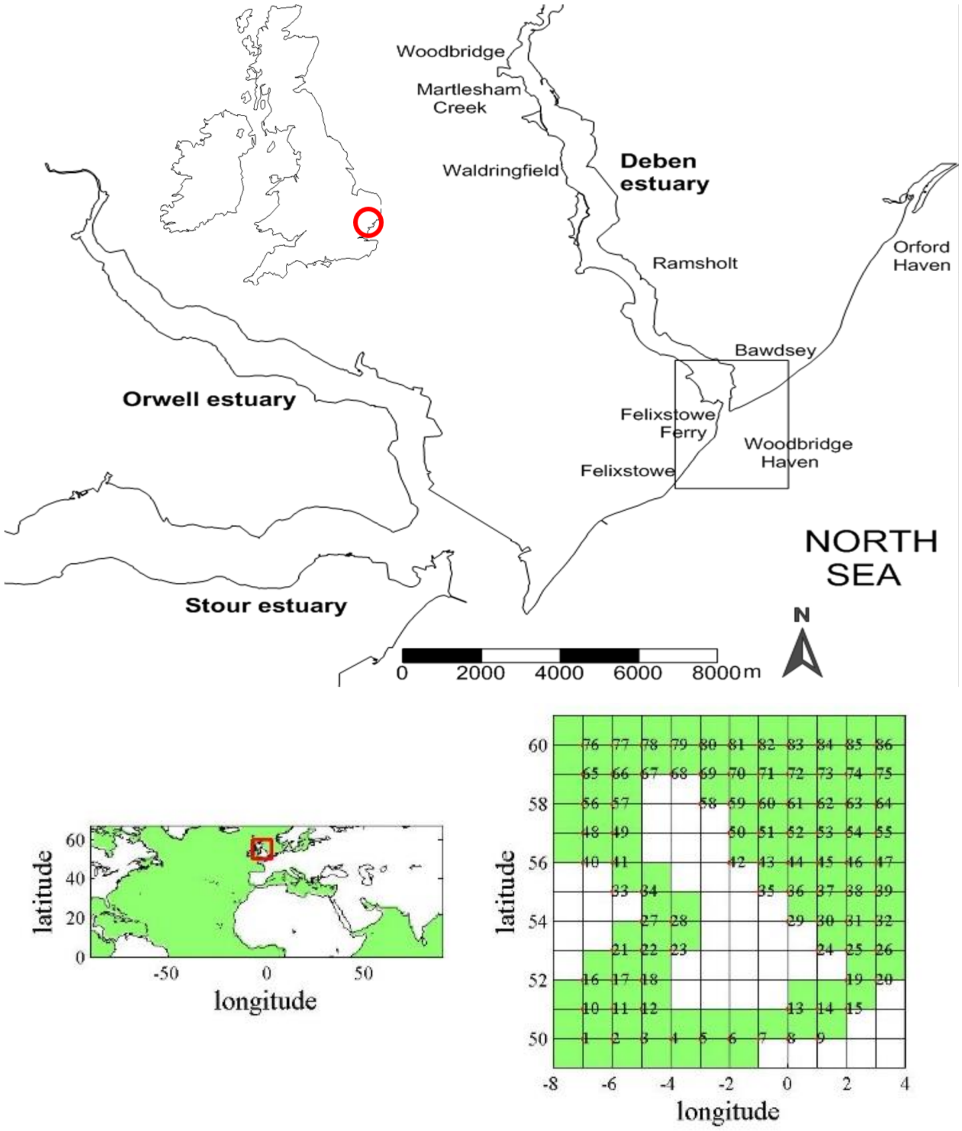

Figure 1. The study area (up) and the global wave model nodes (bottom in green color, node No. 19 was selected in this study)

The sediment medium diameter (D_{50}) distribution is spatially varying across the region. The D_{50} in the main channel is taken as 42.2mm, which is gravel dominated (Burningham and French, 2006). D_{50} at the flood tidal delta is defined as 0.4mm and D_{50} at the ebb tidal delta is assumed to be 7mm with only one fraction for simplification, although it was found that different fractions exist along the exploratory trenches (HR Wallingford, 2002; Burningham and French, 2006). The Bijker (1971) sediment transport equation is selected.

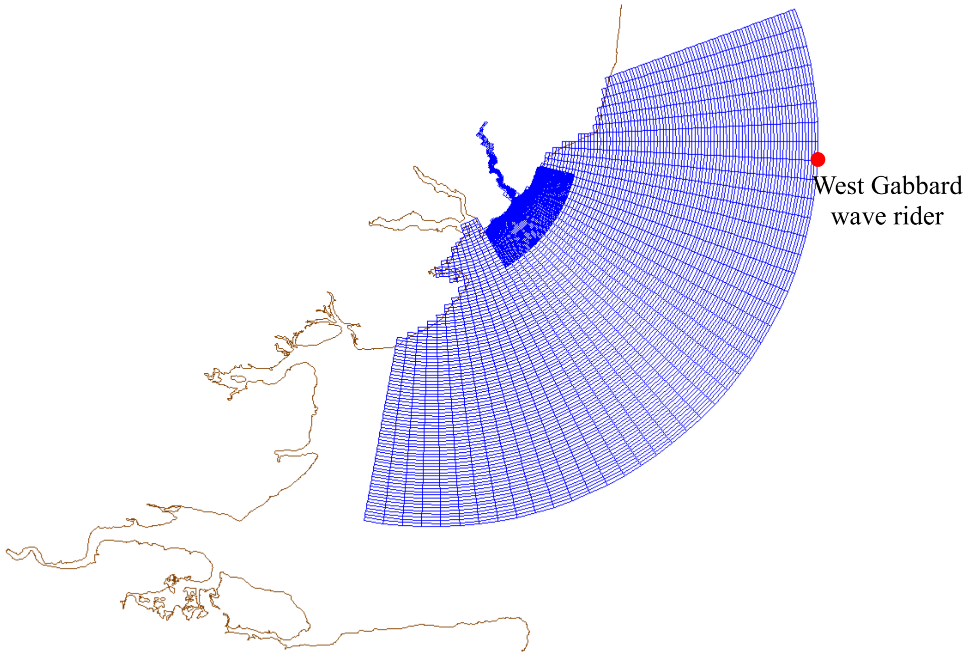

Figure 2. The nested domains for SWAN module and wave rider that used as the boundary condition in this study. The red dot is the location of West Gabbard wave gauge described in text.

2.2. *Probable extreme wave change in the future*

The offshore wave boundary condition was determined from a global wave simulation with WAVEWATCH Ш forced by sea surface wind from the atmospheric climate simulation developed by Japanese Meteorological Research Institute (MRI-AGCM) (Mizuta et al., 2012; Stocker et al., 2013; Shimura et al., 2015). The MRI-AGCM model used different Sea Surface Temperature, (SST), clusters projected by 18 models from Phase 3 of the Coupled Model Intercomparison Project, (CMIP3), as the boundary conditions, (Murakami et al., 2012). In this study, we selected the ensemble-mean SST cluster scenario projected by 18 models of CMIP3. Waves have been simulated over two time slices, one is the 'present' time period from 1979-2009 and the other is the 'future' time period from 2075-2099.

Table 1. The extreme significant wave heights (Hs) in different return periods based on Gumbel regression (Gumbel, 1954).

	10-year return period	20-year return period	30-year return period	50-year return period	100-year return period	200-year return period
Current H_s(m)	6.09	6.41	6.60	6.84	7.16	7.49
Future H_s(m)	6.18	6.51	6.71	6.95	7.28	7.61

Before using the dataset of this global wave simulation, the measured wave data at West Gabbard wave gauge (51°58.96'N, 2°4.91'E) provided by the Centre for Environment, Fisheries and Aquaculture Science (Cefas) wave net, is used to validate the global wave outputs. The location of West Gabbard is also defined as the wave boundary location of our model, (Figure 2). So, the wave dataset at node NO.19 in Figure 1, which was closest to West Gabbard wave gauge, was selected. The validation results have shown that the global model outputs very closely match with the measured data in terms of storm wave heights, peak periods and directions in the current time slice.

The Table 1 shows the present and future extreme wave heights determined from the global wave simulation. The significant wave height with 1 in 100-year return period (1% H_s) is selected as the extreme wave height in this study. Then, an idealized storm profile was developed using a triangular shape by considering both the present extreme wave scenario and future extreme wave scenario when the stationary wave method was used (Figure 3).

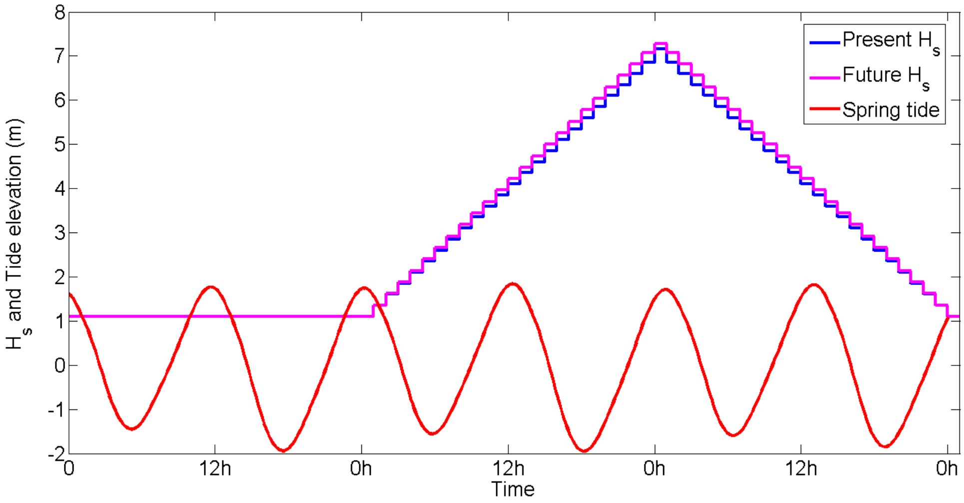

Figure 3. Assumed time series of significant wave height, (H_s), and spring tide conditions for the models in present and future scenarios during the 3-day simulation (from 01/09/2002 00:00am to 04/09/2002 00:00am) and the highest H_s value happens at the time 03/09/2002 00:00 coincident with spring high tide.

It can be seen in Figure 3 that differences in extreme wave height during present and future scenarios are not very large, with an increase in future by approximately 2% from the present scenario. However, such small differences may lead to contrasting morphodynamic responses due to the nonlinear nature of the processes with high energetic tide. Both two sets of simulations carried out in this study are performed under spring tide conditions. So, in this preliminary study, it was considered that the storm coincides with spring tide and the wave storms peak at the spring high tide, to simulate worst case scenarios.

The starting time of all the simulations was taken to be 01/09/2002 00:00am and the simulations lasted for 3 days with gradual increase from mean Hs to 1 in 100-year return period value as shown in Figure 3. The peak wave period T_s was taken as the average wave period from global wave outputs. The incident wave direction was taken as the predominant wave direction determined from the modelled waves, (45^{o}N).

2.3. *Simulated scenarios*

The Deben Estuary exhibits three distinct morphological states between which the ebb tidal delta cyclically evolves, (Burningham and French, 2006). These three important bathymetry states are shown in Figure 4, in which State A is the morphology associated with the progressive extension of the updrift ebb-tidal shoal causing down-drift migration of the ebb-jet and some recession of the downdrift shoreline; State B contains cross-shore breakdown of the updrift shoal and downdrift shoal extension and diversion of the ebb channel; State C has relocated the ebb jet region to a northerly position resulting from a permanent breach of the updrift shoal, (Figure 4). Therefore, different states will be used to determine how these bathymetries will respond to future storms and the difference in response under present and future extreme wave conditions.

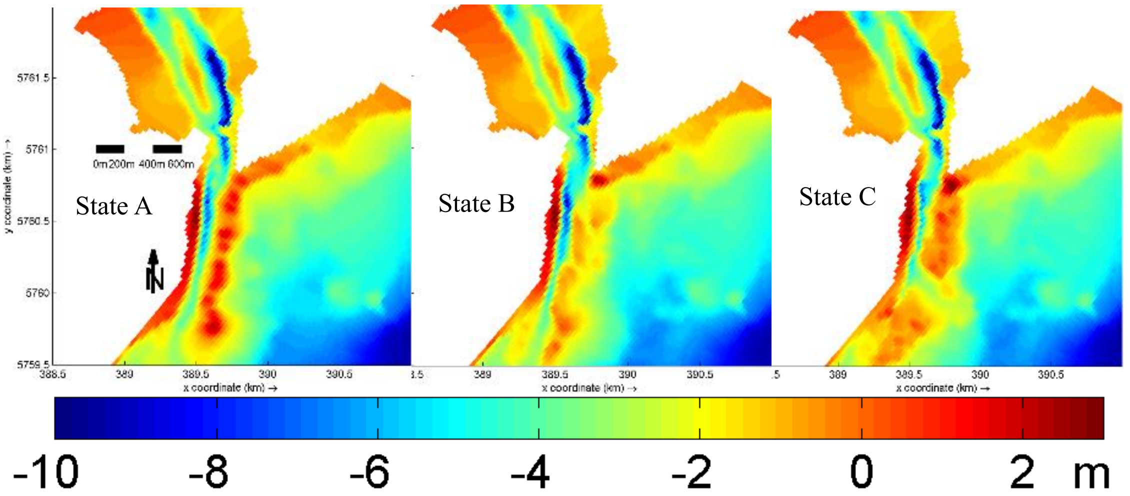

Figure 4. Three representative bathymetry states that used in this study: State A (left); State B (middle); State C (right).

3. Results and discussions

The morphodynamic evolutions of the Deben Estuary under the extreme storm-tide scenarios described in Section 2 are discussed in this section. All the three bathymetry states respond differently to the future wave conditions.

3.1. *State A*

The first selected bathymetry state is State A in which the initial bathymetry contains an elongated ebb shoal paralleling to the south bank coastline and connected to the north shoreline. Most of the ebb shoal is intertidal.

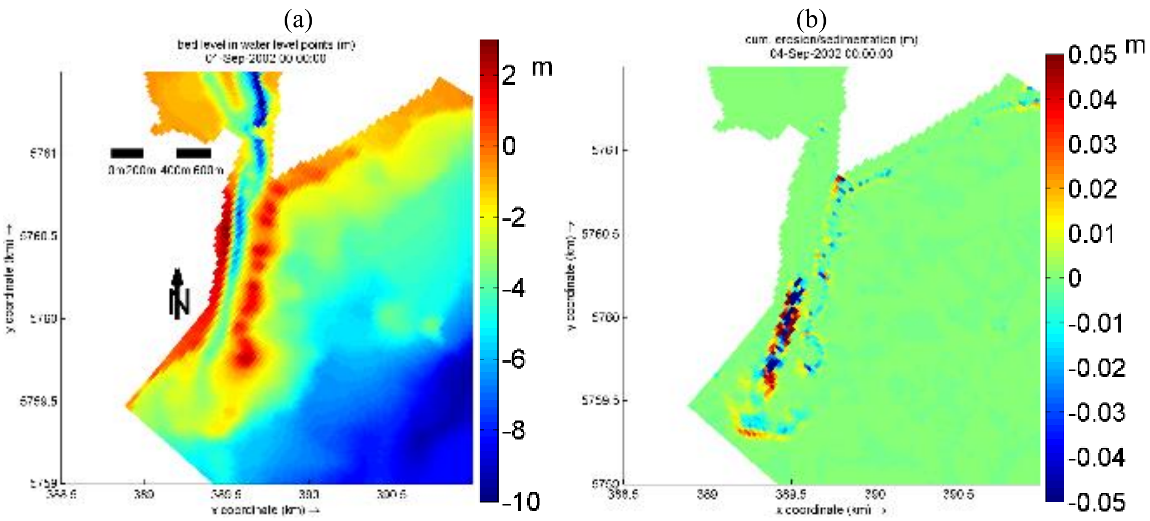

Figure 5. The result in future scenario in State A; a) initial bathymetry; b) the cumulative erosion/sedimentation after simulation under the condition of future1 in 100 year storm wave with spring tide. Negative value means erosion and positive value means accretion.

When the future 1%, (1 in 100 year), storm peak coincides with the spring tide, the most dynamic area in the estuary is found to be the downstream of the main channel as shown in Figure 5b. Apart from the dynamic channel, the south ebb jet region also experiences much more bed level changes with offshore sediment transporting as the Figure 5b shows sediment accretes at the far side of ebb jet region. There is also a clear morphological change at the frontage of south ebb shoal which shows some erosion at this site, (Figure 5b). Apart from the dynamic south part of ebb shoal in this state, the north tip of the ebb shoal which is around the inlet also experiences slight erosion when the future extreme wave condition happens with the spring tide.

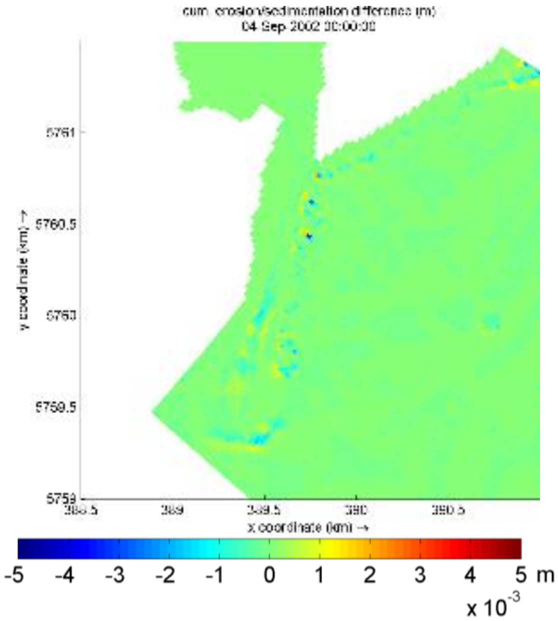

Figure 6. The difference on bed level changes between the present and future scenarios associated with spring tide (future minus present). Negative values indicate that future bed level change is smaller than present bed level change; positive values mean the future change is larger than present one.

It was found that the future 1% storm wave height at the offshore boundary of the model domain is 0,2m larger than that of the present 1% storm wave condition. However, it can be seen that the increase in future wave height closer to the mouth of the estuary is only about 0.02m from the current wave height (increase by around 2.3% from the present scenario). So, the difference between the current and future morphology change of the estuary under 1% storm condition is extremely small, (Figure 6).

Although the difference is negligible for practical purpose when including the numerical errors and uncertainties in sediment transport formula used in model, it provides an indication on which part of the system is the more sensitive to the wave changes. This can be used as a guideline in determining the significant morphological responses if much more intense storms occur.

It can be seen that both the north part of the ebb shoal and the frontage of southern ebb shoal are the most sensitive areas to change in extreme waves when occurring during the spring tide. For the south part of the ebb shoal, the maximum difference is mostly within $\pm 1\times10^{-3}$m while the maximum difference at north part of ebb shoal can reach up to $\pm 2\text{-}3\times10^{-3}$m, (Figure 6), which has been changed by 3% on the bed level change between present and future scenarios. The changes of erosion/accretion pattern at the south part of ebb shoal due to extreme wave change during spring tide only increased by 0.7% based on the present bed level change. So, under the spring tide condition, the most vulnerable position in this system to the extreme wave change will be at north ebb shoal although there is a slight effect from the extreme wave change to the south ebb shoal frontage, (Figure 6).

3.2. *State B*

Another one of the most important representative bathymetry states of the Deben estuary is the one containing a breaking updrift shoal and an extended downdrift shoal, (Figure 7a). The north part of the ebb shoal was broken down into segments much more seriously than the south part and there is a very shallow triangular frontage at the south which may potentially shield the wave propagation or the longshore sediment transport from north.

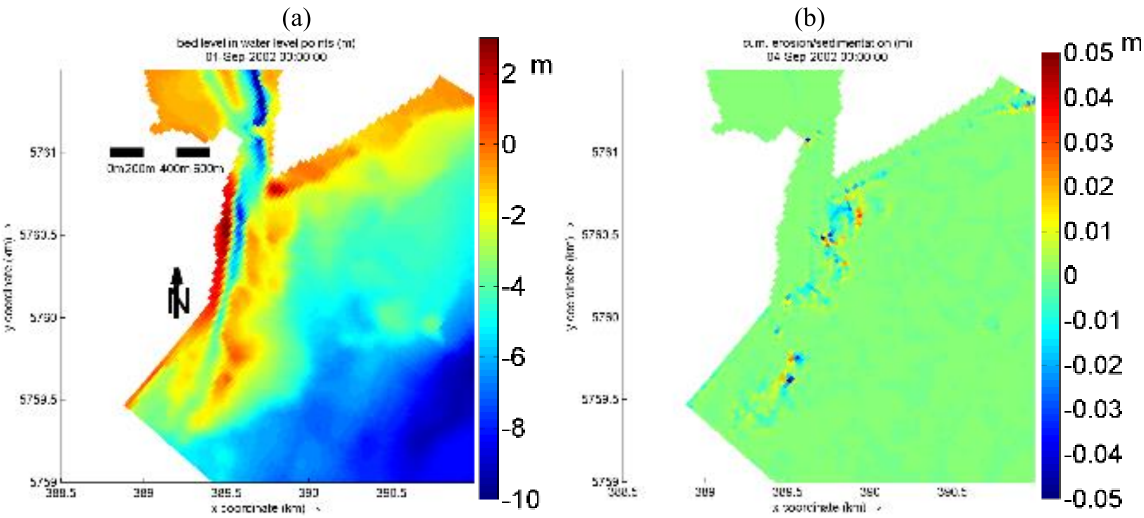

Figure 7. The result in future scenario in State B; a) initial bathymetry; b) the cumulative erosion/sedimentation after simulation under the condition of future 1% storm wave with spring tide. Negative value means erosion and positive value means accretion.

The cumulative erosion and accretion of bed level under the future 1% extreme wave storm coincides with the spring high tide are shown in Figure 7. In this state, although the hydrodynamic inputs are the same as in state A, the morphodynamic responses are different. There is no significant morphological change in the main channel but the changes at the north part of ebb shoal are much stronger than that in state A. In addition, there is a clear dynamic change on bed level at the frontage of the south ebb shoal. So, it seems that both north and south parts of ebb shoal will experience much greater changes, (Figure 7b).

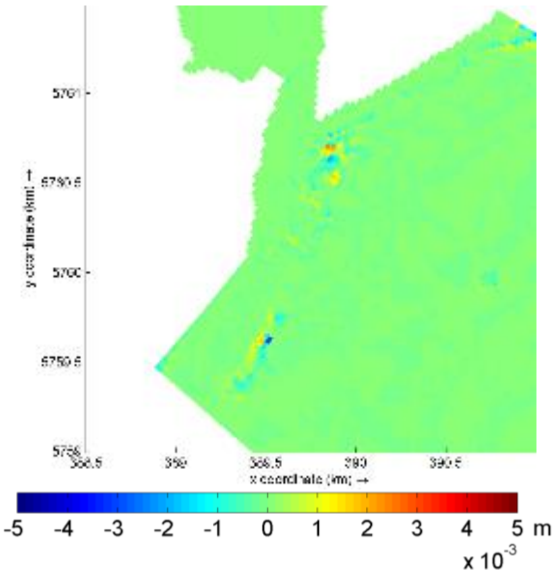

Figure 8. The difference on bed level changes between the present and future scenarios associated with spring tide range (future minus present). Negative values indicate that future bed level change is smaller than present bed level change; positive values mean the future change is larger than present one.

When considering the difference of morphodynamic changes between present and future scenarios, it becomes more obvious than that in state A due to 1% storm wave climate change, (Figure 8). The most sensitive area to extreme wave change in this state is located at both south tip of ebb shoal and north tip of ebb shoal in both of which the bed level is very dynamic under the tide and wave condition, (Figure 7b). Therefore, due to the interaction between currents and waves, the morphology will be much more sensitive to changes in waves or tidal currents in this breaking ebb shoal state.

In terms of bed change difference between present and future extreme wave climates, the difference is more significant than that in State A, which has changed by around 6.7% from the maximum bed change in present scenario. Therefore, the ebb shoal of this state is much more sensitive to the extreme wave change than that in State A.

3.3. *State C*

One of the other main characteristic estuary states (State C), which contains two divided fully formed ebb shoal, is also selected to investigate. The cumulative accretion/erosion pattern under the 1% storm wave conditions associated with spring tide is shown in Figure 9.

In general, the most dynamic area in State C under the condition of future extreme wave with spring tide is mostly limited around the ebb jet region. The channel at the upstream of this region experiences much more erosion and the sediment accretes at the offshore side, (Figure 9). This is likely to be because the local increase in H_s at the ebb jet as the water level increases at the high spring water, (Figure 11), and the significant tidal current at the deep ebb jet region. In addition to the ebb jet region, the north ebb shoal also shows some changes as well in the future scenario, (Figure 9b).

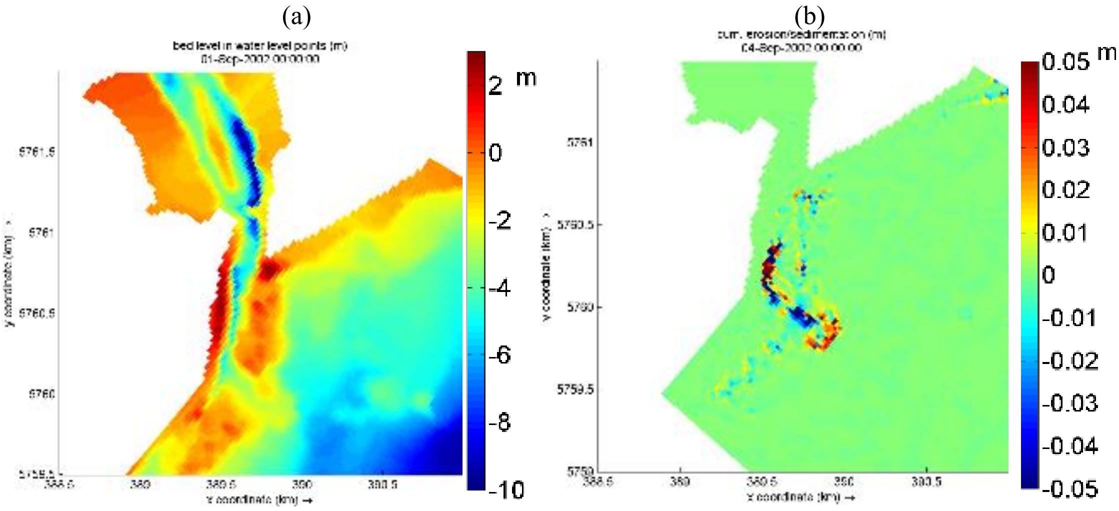

Figure 9. The result in future scenario in State C; a) initial bathymetry; b) the cumulative erosion/sedimentation after simulation under the condition of future 1% storm wave with spring tide. Negative value means erosion and positive value means accretion.

But when considering the bed change differences due to current and future extreme wave change, the increased extreme wave condition did not generate a notable difference during spring tide condition on two ends of the ebb shoal, unlike the previous two states did, but generate a clear difference within the ebb jet region, (Figure 10). The negative values at onshore side and positive values at offshore side shown in Figure 10 indicated that the increase of the extreme wave change will accelerate the offshore sediment transport at the ebb jet region, (Figure 9b). Therefore, the most vulnerable place in this system to the extreme wave change is the ebb jet region while the remaining part of ebb shoal in this state will be much more sustainable to the extreme wave change. The area containing differences is thus not as much as large as the other two states.

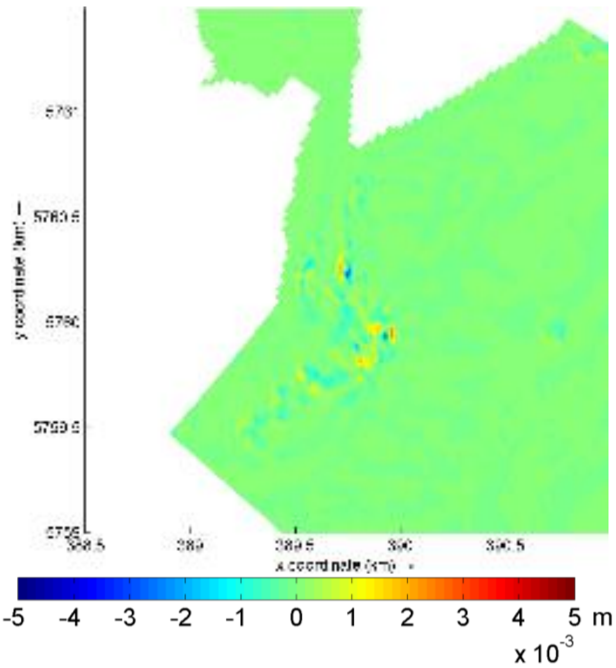

Figure 10. The difference on bed level changes between the present and future scenarios associated with spring tide (future minus present). Negative values indicate that future bed level change is smaller than present bed level change; positive values mean the future change is larger than present one.

However, in terms of maximum bed change difference between present and future extreme wave climates, the future wave condition will alter the bed change by 8.4% from the maximum bed change in present scenario, which is larger than previous states. So, it seems that the range of difference that extreme wave change generates in this state is the most serious among these three states. However, the affected area has reduced significantly. Therefore, it is indicated the change of extreme wave condition may increase the range of sediment erosion and accretion easily in this state, but this significant increase is only restricted within the ebb jet region other than the whole ebb shoal, (Figure 10).

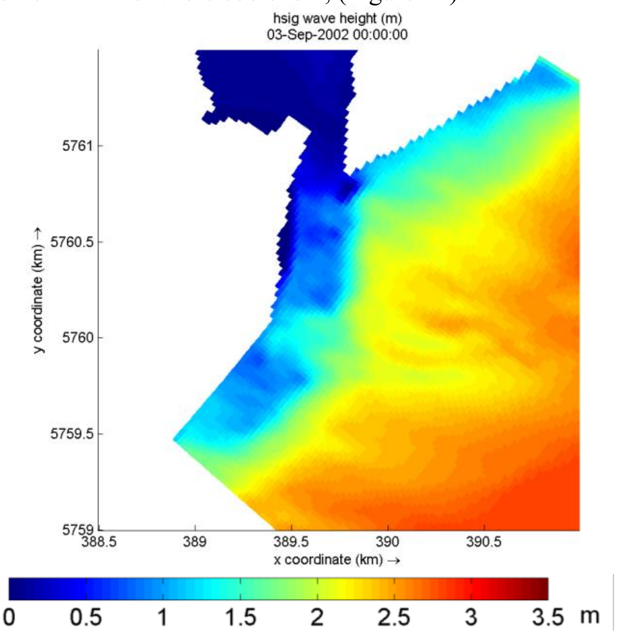

Figure 11. The H_s distribution around the estuary at the time of future 1% storm extrme wave (03/09/2002 00:00am) during spring tide in State C.

4. Conclusion and future work

This study investigated the morphological responses of the Deben Estuary to current and future extreme wave conditions during spring high tide by studying the morphological response of three representative bathymetry states. The morphodynamics at different selected bathymetry states show different sensitivities to the extreme wave change during spring high tide.

For the State A, the most significant bed change happens at the main channel while both north and south tip parts of ebb shoal will also experience a relative high bed level change under the future condition. In State B, the most dynamic place is located at the north part of ebb shoal which is close to the inlet whereas the most dynamic part in State C is at the ebb jet region.

Since the morphodynamic responses vary with extreme wave condition, the morphodynamics at the different selected bathymetry states have shown different sensitivities to the extreme wave change during spring tidal range. In both State A and B, the common morphological changes can be found at the frontage of down-drift beach and north part of the ebb shoal which is most obvious in State B. But the State C shows different situation in which the two end sides of ebb shoal are no long sensitive to the extreme wave change. Instead, the most sensitive place is restricted at the ebb jet region as the ebb jet switches directly to the incident wave direction.

Among these bathymetry states, the most important role that wave can play is in State B, in which there are several breaches existing at the north part of the ebb delta. Within this bathymetry state, the developing ebb delta (contains breaches) seems to be the most vulnerable to the wave change and the most sensitive part is the north ebb shoal. In contrast, the least vulnerable state to wave change is in State C in which the entire ebb shoal will not be affected by extreme wave change except for the ebb jet region.

This paper has presented some preliminary results from different scenarios. More detailed results will be presented in the future, and will explore the importance of water level in determining the morphological response to extreme waves. This includes the effects at lower stage of the tide as well as the impact that sea level rise might have. The latter effect should be considered because sea level rise may affect the nearshore wave transformation characteristics in the future, as suggested by Chini et al. (2010), and thereby alter the morphological response of the estuary.

Acknowledgements

We appreciate the iCOASST project for providing the bathymetry data and British Oceanography Data Centre (BODC) and CEFAS for providing tide and wave data for model validation. We also thank Dr. Nobuhito Mori at Disaster Prevention Research Institute of Kyoto University for providing future projected wave data. The first author would like to thank the China Scholarship Council (CSC) for funding the Ph.D. study in Swansea University. EFRaCC project is acknowledged for the financial support provided for attending Coastal Dynamic 2017 conference.

References

Arnott, W.G., 1968. Suffolk Estuary: The Story of the River Deben. *Norman Adler & Co, Ipswich*. 132 pp.

Beardall, C.H., Dryden, R.C., Holzer, T.J., 1991. *The Suffolk Estuaries*. Segment Publications, Colchester. 77 pp.

Bijker, E., 1971. Longshore transport computation. *ASCE Journal of Waterway, Port, Coastal and Ocean Engineering*, 97: 687-701.

Booij, N., Ris, R., and Holthuijsen, L.H., 1999. A third-generation wave model for coastal regions, Part I, Model description and validation. *Journal of Geophysical Research,* 104 (C4): 7649–7666.

Burningham, H., French, J., 2006. Morphodynamic behaviour of a mixed sand–gravel ebb-tidal delta: Deben estuary, Suffolk, UK. *Marine Geology*, 225(1-4): 23-44.

Chini, N., Stansby, P., et al., 2010. The impact of sea level rise and climate change on inshore wave climate: A case study for East Anglia (UK). *Coastal Engineering*, 57(11-12): 973-984.

DEFRA, 2008. Development and Demonstration of Systems-Based Estuary Simulators. R&D Technical Report FD2117/TR. London: DEFRA.

Delf3D Wave User Manual, 2014. http://oss.deltares.nl/web/delft3d/manuals.

Dissanayake, P. K., 2011. Modelling Morphological Response of Large tidal inlet system to Sea Level Rise, Ph.D theis.

Gumbel, E.J., 1954. Statistical theory of extreme values and some practical applications: a series of lectures. Applied Mathematics Series. 33 (1st ed.). U.S. Department of Commerce, National Bureau of Standards

Hasselmann, K., Barnett, T.P., et al, 1973. Measurements of Wind-Wave Growth and Swell Decay during the Joint North Sea Wave Project (JONSWAP). Hamburg.

HR Wallingford, 2002. Southern North Sea Sediment Transport Study (phase 2). HR Wallingford Report EX, pp.4526.

Lesser et al., 2000. On-line sediment transport within Delft3D-FLOW, Delft Hydraulic.

Lesser, G., Roelvink, J., van Kester, J., and Stelling, G., 2004. Development and validation of a three-dimensional morphological model. *Coastal Engineering*, 51(8-9): 883-915.

Mizuta, R., and Coauthors, 2012. Climate simulations using MRI-AGCM3.2 with 20-km grid. *Journal of the Meteorological Society of Japan*, 90A: 233-258.

Murakami, H., Mizuta, R., Shindo, E., 2012. Future changes in tropical cyclone activity projected by multi-physics and multi-SST ensemble experiments using the 60-km-mesh MRI-AGCM. *Climate Dynamics*, 39: 2569-2584.

Posford Duvivier, 1999. Suffolk Estuarine Strategies: Deben Estuary. Strategy Report: Phase 2 volume 1 Main Report. Peterborough: Environment Agency: Anglian Region, pp. 5-20.

Shimura, T., Mori, N., Mase, H., 2015. Future projection of ocean wave climate: analysis of SST impacts on wave climate changes in the Western North Pacific. *Journal of Climate,* 18: 3171-3190.

Stocker, T. F., and Coauthors, 2013. Climate change 2013: *The Physical Science Basis. Cambridge University Press*, pp. 1533.

Taylor, J.A., Murdock, A.P., Pontee, N.I., 2004. A macroscale analysis of coastal steepening around the coast of England and Wales. *The Geographical Journal*, 170 (3): 179– 188.

van der Wegen and Roelvink, 2012. Reproduction of estuarine bathymetry by means of a process-based model: Western Scheldt case study, the Netherlands. *Geomorphology*. 179: 152-167.